

Hardware Considerations for Functional Magnetic Resonance Imaging

AFONSO C. SILVA, HELLMUT MERKLE

Laboratory of Functional and Molecular Imaging and NIH MRI Research Facility, National Institute of Neurological Disorders and Stroke, National Institutes of Health, 10 Center Drive, Building 10/B1D118, Bethesda, Maryland 20892-1065

ABSTRACT: Functional magnetic resonance imaging (fMRI) techniques based on changes in blood oxygenation or regional cerebral blood flow or volume have had great impact in mapping the regions of the brain that are activated by specific stimuli. The basic strategy of fMRI paradigms is to acquire data during two different brain states: one state usually comprises a resting condition, while in the other state the subject is performing a specific sensory or cognitive task. The signal difference between the activated and resting signals is on the order of only a few percent, and therefore the reliability and reproducibility with which it can be detected limit both the temporal and spatial resolution of fMRI experiments. The era of fMRI has significantly contributed to advancing the state of the art of MRI scanners. Every hardware component in modern MRI scanners, from the magnet itself to the gradient, shim, and RF coils to peripheral stimulus delivery equipment, has been (re)designed to perform to the limit of currently available technology and to improve the quality of MRI data, particularly fMRI data. The current state of the art of MRI scanners is described in light of their use in fMRI experiments. © 2003 Wiley Periodicals, Inc. *Concepts Magn Reson Part A* 16A: 35–49, 2003

KEY WORDS: hardware; functional magnetic resonance imaging; blood oxygenation level dependence; cerebral blood flow and volume

INTRODUCTION

Since the first experiments in the early 1990s, functional magnetic resonance imaging (fMRI) techniques

Received 19 September 2002; accepted 1 October 2002

Correspondence to: Dr. H. Merkle; E-mail: merkleh@ninds.nih.gov.

Concepts in Magnetic Resonance Part A, Vol. 16A(1) 35–49 (2003)

Published online in Wiley InterScience (www.interscience.wiley.com). DOI 10.1002/cmr.a.10052

© 2003 Wiley Periodicals, Inc.

based on either changes in blood oxygenation level dependence (BOLD) (1, 2), regional cerebral blood flow (rCBF) (3, 4), or regional cerebral blood volume (rCBV) (5) have had great impact in mapping the regions of the brain that are activated by specific stimuli. The basic strategy of fMRI paradigms is to acquire data during two different brain states: one state usually comprises a resting condition, which defines the baseline fMRI signal, in which the subject is either resting or performing tasks unrelated to the task of interest. The second state occurs during performance of a specific sensory or cognitive task, and it defines the “activated” signal. The signal difference

between the activated and resting signals is on the order of only a few percent, and therefore the reliability and reproducibility with which it can be detected limit both the temporal and spatial resolution of fMRI experiments. It is fair to say that fMRI has significantly pushed the advancement of the state of the art of MRI scanners, because the higher the quality of the hardware performing the data acquisition, the higher the quality of the data itself. Every hardware component of modern MRI scanners, from the magnet itself to gradient and shim coils, RF coils, and receiver chains, has been designed or redesigned to perform to the limit of currently available technology and to improve the quality of MRI data, in particular fMRI. It is the purpose of this article to describe the current state of the art of MRI scanners in light of their use in fMRI experiments. The information included here is in many respects complementary to that given in (6). Consideration is given to the major elements of a modern MRI scanner, including the magnet, the gradient and shim coils, the RF coils, and the receiver preamplifiers. We also elaborate on the peripheral equipment necessary for stimulus delivery and physiological monitoring. Finally, we comment on future directions for fMRI hardware development.

HARDWARE COMPONENTS OF MODERN fMRI SCANNERS

Superconducting Magnet

The magnet is the main element of an MRI scanner. It generates a strong and homogeneous magnetic field, which polarizes MR-detectable nuclei such as ^1H . The magnet is composed of a large solenoid coil, which is wound from superconducting wires that hold the large current densities necessary to generate the magnetic field. Additional superconducting shimming coils are wound on top of the primary coil to correct field distortions and improve homogeneity. Superconducting wires operate at very low temperatures but safely below the boiling temperature of helium (4.2 K or -269°C), and therefore the main solenoid sits in a cryostat submerged in a bath of liquid helium. The cryostat is isolated from room temperature (RT) by a vacuum canister, an optional liquid nitrogen jacket, another vacuum canister, and one or more layers of radiation shield that prevent heat exchange with the outer environment.

The physical dimensions of the magnet are determined by its purpose: dedicated magnets for use with animals range from 89 to 650 mm in free accessible bore diameter; magnets for use with humans vary



Figure 1 The 7-T 900-mm clear bore fMRI magnet used for human research at the University of Minnesota. The view is from the operator console through a screened window into the iron- and RF-shielded magnet room. A patient bed and a whole-body shim and gradient coil assembly is installed in the magnet. An insertable head gradient set can be seen on a cart outside the magnet. The operating room contains all controls for executing MR experiments, paradigm presentation, and patient communication. Picture courtesy of Prof. Kâmil Uğurbil, University of Minnesota. [Color figure can be viewed in the online issue, which is available at www.interscience.wiley.com.]

from 800 mm to as much a 1250 mm in bore diameter. Figure 1 shows a state of the art 7-T 900-mm magnet used for fMRI and MR spectroscopy research of human subjects. Siting or placement of an MRI magnet is strongly affected by its field strength, as well as its physical dimensions. Wider bores yield more homogeneous magnets but significantly add to the cost, weight, and siting requirements. The length of the magnet is an equally important parameter used by magnet designers to meet the stringent magnetic field homogeneity (<5 ppm) specifications. Usually human magnets referred to as “whole-body” magnets are 2–3 m long, and they can accommodate a large region of the human body within their homogenous region. With the recent growth of fMRI came the development of dedicated head-only magnets, which are significantly shorter (~ 1.2 m) and narrower (bore diameter ~ 600 mm) than their whole-body counterparts. These magnets are considerably easier to site because of their lower weight and contained fringe field, but they are also less homogeneous.

Magnetic Shielding

The magnetic field generated by MRI magnets needs to be confined to as close to the magnet as possible. Magnetic shielding significantly eases siting of the

magnet and provides for safer operating conditions. Several magnetic shielding configurations are available to contain magnetic fringe fields. Passive magnetic shielding of the magnet can be accomplished by a symmetric iron structure weighing up to several hundred tons that is placed around the magnet. This structure can encase the magnet tightly in a configuration referred to as a “closely coupled” shield or encase the entire magnet room. Recent technological developments have allowed the manufacturers to utilize active shielding of the magnet. This is accomplished by winding a superconducting coil outside the main solenoid coil to counteract the main magnetic field outside of the magnet. Passive and active shielding are very efficient in containing the fringe fields to within a few meters from the center of the magnet.

Magnet Shimming and RT Shim Coils

The homogeneity of the magnetic field generated by a magnet is a crucial parameter for obtaining high-quality images. Typical MRI magnets are homogeneous to within 5 ppm over a predetermined spherical volume of interest located in the center of the magnet. Magnet manufacturers resort to several strategies to optimize homogeneity upon installation and energization of the magnet. Cryoshimming utilizes a set of auxiliary second- and third-order superconducting coils, which are wound over the main magnet solenoid. Permanent DC currents are applied to the superconducting shim coils by iteratively plotting the field profiles along many points inside a spherical volume and adjusting the currents until homogeneity specifications are achieved. In some instances, passive shimming is also used in addition to cryoshimming to aid the achieving of homogeneity specifications. Like cryoshimming, passive shimming is also performed only once upon installation of the magnet by carefully positioning trays containing pieces of ferromagnetic metal along the bore of the magnet. Whenever possible, fMRI-dedicated magnets should avoid the use of passive shim trays inside the free bore of the magnet, because of temperature variations induced by heating of the gradient coils. A change in temperature of the bore changes the magnetic property of the ferromagnetic shims, inducing B_0 drifts that affect the time course of the fMRI signal.

Whereas cryoshimming and ferroshimming are performed to correct the intrinsic inhomogeneities of the magnet, it is also necessary to shim-out the inhomogeneities introduced by the presence of the subject in the magnet. For this purpose, a resistive set of shim coils is installed inside the magnet bore. The shim coils are carefully wound to produce specific field

patterns based on spherical harmonic functions, which can range from first to fifth order. The RT shim coils are fed by a multichannel DC current amplifier, which is computer controlled to individually adjust the current on each RT shim coil. Adjustment of the homogeneity using RT shims can be accomplished manually or by means of an automated software program, such as FASTMAP (7), which optimizes homogeneity over a localized region of the brain. RT shimming makes it possible to correct inhomogeneities that vary from one subject to another and that may severely affect the quality of the fMRI images. Therefore, RT shimming is an important preacquisition component of fMRI experiments.

Gradient Coils

MR images are produced by a 3-dimensional (3-D) spatial encoding of the signal from the region of interest. This is accomplished by superimposing to the main, homogeneous magnetic field a linear field variation along the three Cartesian axes X , Y , and Z . When data is being acquired in an MRI scanner, current waveforms are pulsed into the gradient coils to generate the field gradients. Gradient coils are copper windings shaped into specific patterns and plotted around a cylindrical former, including an outer assembly of shield coils especially designed to minimize field gradients outside the shield. The gradient coil assembly also includes pipes containing circulating refrigerated water for removal of heat generated by ohmic losses, and temperature sensors are embedded in several points of the gradient coil assembly. In many cases, the RT shim coil assembly is an integral part of the gradient coil assembly.

An effective inductance (L_G) and resistance (R_G) electrically characterize the gradient coils. Both L_G and R_G are a function of the coil geometry and are determinants of the performance of the gradient set. Such performance is measured by how strong gradient amplitudes can be produced, how fast they can be achieved, and how often they can be repeated. These three parameters are highly dependent on the coil geometry, and several different design approaches have been proposed over the last 20 years to improve the overall performance of gradient coils. [For a review, see (8).]

The maximum gradient strength G_{\max} ($\text{mT} \cdot \text{m}^{-1}$) is a product of the coil efficiency η ($\text{mT} \cdot \text{m}^{-1} \cdot \text{A}^{-1}$) and the maximum current amplitude I supplied by the gradient amplifiers. The coil efficiency is mostly influenced by its geometry: the smaller the diameter and the smaller the inductance, the more efficient the coil is and vice versa. Whole-body gradient sets, which are

always in place inside the magnet and allow for an easy experimental setup, come in inner diameters ranging from 63 to 72 cm and can produce a G_{\max} up to $40 \text{ mT} \cdot \text{m}^{-1}$. Although this peak gradient strength is quite sufficient for the echo-planar imaging (EPI) typically used in fMRI experiments, whole-body gradient coils are largely inefficient and slow, because they have large inductances. Because of this, some human fMRI instruments are equipped with a head-only insertable gradient set. This set mounts inside the whole-body gradients and typically has a 32–38 cm inner diameter. Head-only inserts are significantly more efficient than whole-body gradients, allowing very high performance for fast scanning, thus making them quite attractive for fMRI experiments. Typically, head-only inserts can produce up to 65 mT m^{-1} in a significantly shorter rise time than a whole-body gradient set. In small animal gradient sets, the G_{\max} can reach 1000 mT m^{-1} .

The gradient rise time, defined as the time necessary to reach maximum gradient amplitude, is a function of the L_G and R_G of the coil, the maximum I , and the voltage compliance V supplied by the gradient amplifiers:

$$\tau = \frac{L_G \times I}{V - R_G \times I} \quad [1]$$

Another way of evaluating the performance of a gradient coils is to obtain a measure of the slew rate ($\text{T} \cdot \text{m}^{-1} \cdot \text{s}^{-1}$), which is defined as

$$S = \frac{G_{\max}}{\tau} = \frac{\eta \times I_{\max}}{\frac{L_G \times I_{\max}}{V - R_G \times I_{\max}}} = \frac{\eta \times (V - R_G \times I_{\max})}{L_G} \quad [2]$$

It can be seen from Eqs. [1] and [2] that the L_G of the gradient coils has an adverse effect on the rise time (or the slew rate), so that most gradient-design approaches employ an inductance minimization constraint as a way to improve performance. Another strong factor influencing the performance of gradients is the power of the gradient amplifiers used to drive the gradient coils. Recently, there has been significant progress in the development of new gradient amplifiers, which are now capable of supplying currents in excess of 500 A with voltage compliances of 2000 V. This new class of amplifiers has been a great contributor to the advancement of fMRI.

The gradient duty cycle is a measure of how often currents can be pulsed and sustained into the gradient coils. It is effectively limited by heat generated

through ohmic losses in the coil wires, and therefore the cooling efficiency of the water pipes is a strong factor in influencing the attainable duty cycle. Usually gradients are built to sustain a 100% duty cycle (i.e., DC currents) at only about 5–10% of the maximum specified current. Peak currents, on the other hand, can only be sustained at 15–25% duty cycles.

RF Coils

These coils are resonant electric structures through which the volume of tissue to be image is excited and the resultant induced MR signal is detected. Therefore, two main features are of interest when designing and building RF coils: it should produce a homogeneous B_1 profile during transmission for uniform excitation of the volume of interest, and it should have high sensitivity during reception for an improved signal to noise ratio (SNR). These requirements are not always mutually attainable, and therefore different coil designs are optimized according to the specific applications. For example, some fMRI experiments attempt to collect information over the entire brain and thus benefit from the use of large, homogeneous volume coils. Other experiments focus on a smaller, particular area of the brain, and these experiments benefit best from the use of small surface coils that are very sensitive but have limited spatial coverage. The fMRI coils need to fulfill additional requirements that need to be incorporated into their design. In particular, fMRI coils are built with special features, such as acoustically insulating padding, which helps minimize interference from acoustical noise; an opening for eye gear or mirrors to allow stimulus presentation in fMRI of the visual cortex or visually cued experiments; and built-in fixtures to aid with head stabilization, such as bite bars. Examples of commercially offered RF coils customized for fMRI studies are shown in Figures 2, 3, and 4.

Volume RF Coils. Volume coils are circumscribing structures that exhibit a highly homogeneous RF field in the volume of interest but typically have a poor filling factor, thereby presenting a compromised SNR. Volume coils can comprise built-in body resonators or whole-head coils. The use of a whole-head coil in transmit or receive mode is the most popular setup utilized for fMRI imaging studies of the whole brain, because it is simple to implement and the SNR is sufficiently high, and thus there is a variety of different head coil designs available from the system vendor or from third-party suppliers. A list of suppliers is included in Table 1. Such coils are optimized for uniform excitation and are driven in quadrature mode

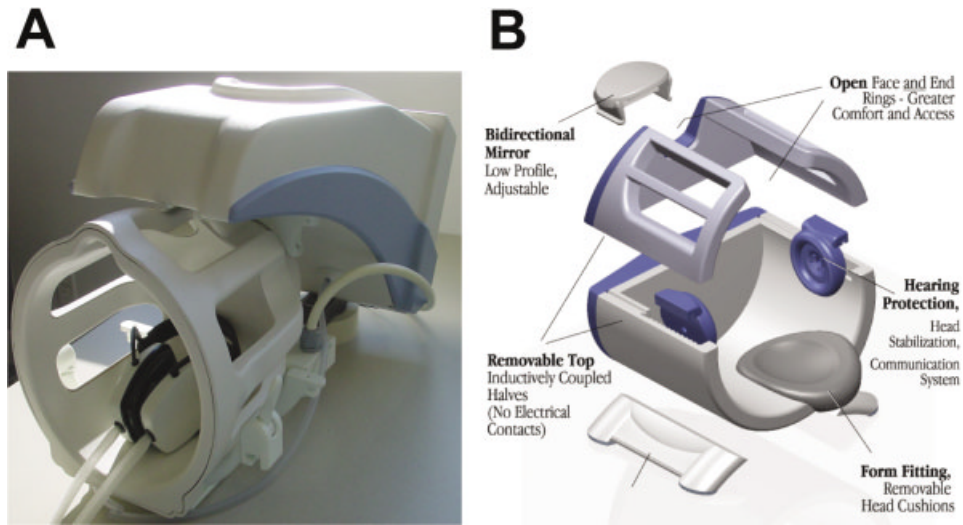


Figure 2 Commercially offered quadrature transceive brain coils, customized for fMRI studies. Coil assemblies include head stabilization devices, earphones or ear protection for communication and presentation of auditory cues, and mirrors for presentation of visual paradigms. (A) Picture courtesy of MRI Devices Corp. (Table 1, vendor 14). (B) Picture courtesy of MR Instruments Inc. (Table 1, vendor 15). [Color figure can be viewed in the online issue, which is available at www.interscience.wiley.com.]

for decreased power during transmission and an improved SNR during reception. The use of a quadrature drive also helps alleviate inhomogeneity associated with dielectric losses, a problem that occurs with great severity at high fields (see below). Typical designs for volume coils include low-pass or high-pass birdcage coils, saddle coils, or transverse electromagnetic resonators.

Surface RF Coils. Unlike volume RF coils, surface coils are small resonant loops designed to pick up the

signal from a limited area. The SNR of surface coils is significantly higher than the one obtained with volume coils, mainly for two reasons. First, because surface coils can be placed directly over the region of



Figure 3 A whole brain transceive coil and head phantom offered within a commercial package. The package includes paradigm presentation, communication gear, and head stabilizing attachments. The coil is curved toward the superior portion of the head for increased sensitivity in that region. Picture courtesy of MRI Devices Corp. (Table 1, vendor 14). [Color figure can be viewed in the online issue, which is available at www.interscience.wiley.com.]

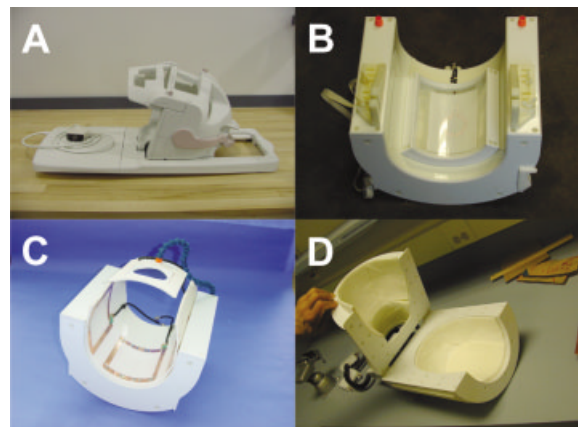


Figure 4 Examples of commercially available brain coils for fMRI experiments. (A) A transceive quadrature whole brain coil, (B) TORO partial volume transmit and single surface receive coils, (C) a four channel transceive coil, and (D) an eight channel gapped receive array for whole brain fMRI. Pictures courtesy of (A) USA Instruments Inc. (Table 1, vendor 29), (B) MR Instruments Inc. (Table 1, vendor 15), (C) University of Minnesota, and (D) NOVA Medical Inc. (Table 1, vendor 18). [Color figure can be viewed in the online issue, which is available at www.interscience.wiley.com.]

Table 1 List of Vendors Providing fMRI Related Products

Vendor	Internet or E-Mail
1. Avotec Inc.	www.avotec.org
2. Bruker BioSpin MRI GmbH	www.bruker-biospin.de
3. Cambridge Research Systems Inc.	www.crsLtd.com
4. Copley Controls Corp.	www.copleycontrols.com
5. Doty Scientific, Inc.	www.dotynmr.com
6. General Electric Medical Systems Inc.	www.gemedicalsystems.com
7. Insight Neuroimaging Systems, LLC	www.insightneuroimaging.com
8. Magnex Scientific Ltd.	www.magnex.com
9. Medrad	www.medrad.com
10. Med-Tech Systems, Ltd.	www.medtechsystems.com
11. Mueller-BBM	www.MuellerBBM.de
12. IGC Medical Advances	mrcoils@medadv.com
13. MRC Institute of Hearing Research	www.ihr.mrc.ac.uk
14. MRI Devices Corp.	www.mridevices.com
15. MR Instruments Inc.	info@mrinstruments.net
16. MR Research Systems	www.mrrs.co.uk
17. NEUROSCAN	www.neuro.com
18. NOVA Medical Inc.	www.novamedical.com
19. Oxford Magnet Technology Ltd.	www.omt.co.uk
20. RAPID Biomedical GmbH	www.rapidbiomed.de
21. Philips Medical Systems	www.medical.philips.com
22. Resonance Technology Inc.	www.mrvideo.com
23. ScanMed	www.scanmed.com
24. SensoMotoric Instruments, Inc.	www.smi.de
25. Siemens Medical Systems	www.siemensmedical.com
26. Source Signal Imaging Inc.	www.sourcesignal.com
27. Tesla Engineering Limited	www.tesla.co.uk
28. Toshiba Medical Systems	www.medical.toshiba.com
29. USA Instruments Inc.	www.usainstruments.com
30. Varian Inc.	www.varianinc.com
31. Wang NMR Inc.	www.wangnmr.com
32. XLResonance	www.xlresonance.com

interest, the filling factor is greatly improved and thus the coil sensitivity increases. Second, because of the limited coverage area, noise contribution is reduced. The disadvantage of surface coils with respect to volume coils is that they possess a rather inhomogeneous field profile; hence, the image intensity varies significantly in space, being significantly lower in regions situated away from the coil. Therefore, it is best to use surface coils as receive-only elements and a volume coil is used for excitation. In this case, the use of special active decoupling hardware is necessary to enable the volume coil and detune the surface coil during the excitation phase of the experiment and to detune the volume coil and tune the surface coil during the receive phase. Electronic tuning and detuning of RF coils is usually accomplished with the aid of pin diodes, which are semiconductor elements that work as logic-controlled RF switches. These diodes are placed either in parallel to the main tuning

capacitor of the resonant loop or in series in the resonant loop in between the tuning capacitor and the coil itself.

MRI Spectrometer

The modern MRI spectrometer is a multiprocessor system that communicates with the host computer to receive instructions and commands, as well as transfer the acquired data at the end of an experiment. The main task of the spectrometer is to generate and execute a sequence of timed events, such as gradient waveforms and RF pulses, and to digitize and store the data prior to sending it to the host computer. The basic units of a modern MRI spectrometer are the following:

1. *Communications unit*: This unit is responsible for communicating with the host computer and

handling the flow of commands and data transfer.

2. *Timing unit:* The timing unit is responsible for generating the timing and order of events during the pulse sequence and maintaining synchronization between multiple events.
3. *Frequency unit:* The unit is responsible for setting the operating frequency and for handling frequency and phase offsets associated with multiple slices, readout offsets, the phase of the RF pulses, and so forth. The output of the frequency unit goes to the RF amplifiers, which drive the RF coils through the transmit/receive (T/R) switch.
4. *Gradient controller:* This controller is responsible for generating and playing gradient waveforms. These waveforms are sent in digital form to the gradient amplifiers, which converts them into streams of analog currents that drive the gradient coils.
5. *Shim controller:* It is responsible for generating and setting current values for the room-temperature shim coils. Currents are amplified by the shim power supply and sent to the shim coils.
6. *Receiver unit:* The receiver unit is responsible for digitizing the data and storing it prior to transfer to the host computer. It receives its input from the RF preamplifiers, which amplify the MRI signals (μV) from the RF coil to a range of a few volts with a low noise figure. Once the data is digitized, it is stored temporarily in banks of memory prior to being transferred to the host computer.

Figure 5 shows a simplified schematic diagram of a typical MRI spectrometer. MRI vendors have taken advantage of the fast and sharp technological developments in electronics over the past decades to push the state of the art in architectural design of MRI consoles. This is one of the main reasons for the improved quality of fMRI data, which demands very high stability, repeatability, and reproducibility of the spectrometer.

CURRENT ISSUES FOR fMRI DEDICATED HARDWARE

Optimal Field Strength for fMRI

Several factors influence the choice of field strength for fMRI. The driving factor is the effective SNR available for a desired spatial and temporal resolution.

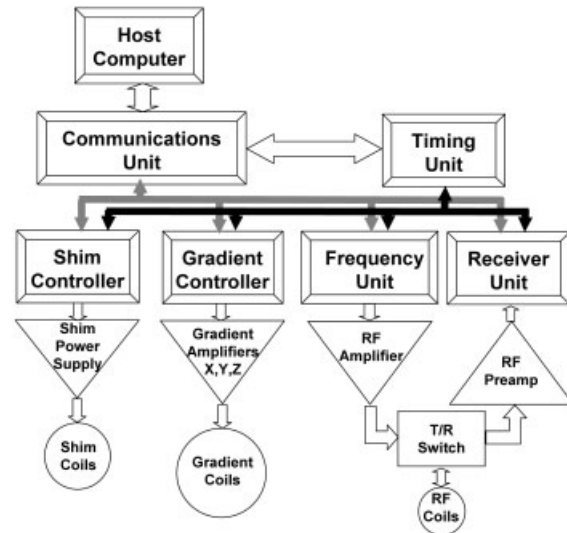


Figure 5 A simplified schematic diagram of a modern MRI spectrometer, which is a multiprocessor system that communicates with the host computer to receive instructions and commands and to transfer the acquired data at the end of an experiment. The main task of the spectrometer is to generate and execute a sequence of timed events, such as gradient waveforms and RF pulses, and to digitize and store the data prior to sending it to the host computer. Please refer to the text for a description of the major blocks.

In the absence of relaxation terms, the SNR increases in linear proportion with the intensity of the magnetic field B_0 (9). This relationship takes into account the NMR signal electromotive force induced in the receiving RF coil, divided by the thermal noise originating from random Brownian electronic motion within the brain tissue and within the RF coil itself. The BOLD contrast to noise ratio (CNR) also increases with the field strength (10). In addition, the spatial localization of the BOLD signal changes is higher at high magnetic fields (please refer to other articles in this issue). Therefore, both the SNR and CNR argue that fMRI should be performed at the highest available magnetic field strength.

However, there are several trade-offs to be considered before opting for a high magnetic field magnet. These include increased RF power deposition, RF inhomogeneity due to eddy-current and wavelength effects, increased acoustical noise from the gradients, reduced anatomical contrast as the longitudinal relaxation time (T_1) increases and the transverse relaxation time (T_2) decreases with the field, increased chemical shift artifacts, and higher physiological noise. In addition, the acquisition, installation, and running costs are significantly higher for high field magnets.

As the magnetic field strength increases, the RF power deposited in the subject by the RF coil in-

creases with a nonlinear dependence that approximates a quadratic curve for $B_0 < 3$ T, increasing less rapidly at higher fields (11, 12). Tissue heating can occur due to repeated RF pulsing into the head, and therefore regulatory agencies have limited the average deposited power into the head to less than 3.2 W/kg. All MRI spectrometers used in humans must have a hardware device that samples the transmitted RF power and shuts off the RF amplifier in case it exceeds the allowed limit. At high magnetic fields, biological tissue can be seen as a lossy dielectric material, which shortens the RF wavelength and causes RF eddy currents (11), thus severely altering the B_1 homogeneity profile of the RF coil. These dielectric resonances cause intensity distortions, and the center of the images usually displays a much higher intensity than the extremities. This problem is somewhat visible at 4 T but really evident at 7 T or higher fields (13).

Gradient Issues

Acoustic Noise. Lorentz forces opposing the change in current in gradient wires or plates cause acoustic noise (14, 15). The tube will act like a loudspeaker membrane when pulsed current flows through the wires. Gradient acoustic noise depends on the pulse sequence used (e.g., on the shape, slope, amplitude, and number of gradient pulses per time), as well on the gradient tube design. The mechanical elasticity module and dimension of the tube determine the modes of acoustic resonances generated in response to a gradient pulse. The mechanically selected acoustic waves propagate within the tube with a number of modes, depending on the electric input function, geometry, and material of tube substrate (e.g., epoxy fiberglass compounds with added fillers for reinforcement). These resonances (movement of substrate) can cause modulations in the apparent electric impedance. These nonlinear characteristics can interfere with electric regulation parameters and therefore degrade gradient performance.

Acoustic noise originating from gradient action is a nuisance to regular imaging, because it causes additional stress to the patient or volunteer. Functional imaging studies typically require pulse sequences that utilize even stronger gradients with higher duty cycle and longer duration compared to anatomical imaging. Acoustic noise can cause functional signals in the auditory cortex, which may interfere nonlinearly with other functional imaging modalities (16–19). Methods to minimize noise are therefore very important (20). Some of the strategies to minimize acoustic noise are now presented.

1. *Pulse sequence design:* Conventional pulse sequences can be modified to use softer gradient waveforms with shaped pulses (e.g., sinusoidal waveforms), which have rounded slopes and therefore a gentler change of current, as compared to conventional trapezoidal or step waveforms. Fourier analysis of shaped waveforms show they contain fewer components at lower frequencies than the traditional waveforms and thus generate less noise. One disadvantage of using shaped waveforms is that they require additional time, which may be a stiff penalty at high fields (21, 22, 65).
2. *Gradient coil design:* Gradient coil designs with intrinsically low acoustic noise have been suggested and built within a research environment (14, 23–27). However, no breakthrough has yet been made in rectifying space constraints, imperfections in eddy current compensation (shielding), and difficulty of manufacturing to allow for practical use of this design in human applications.
3. *Passive damping of noise source:* Insulating and absorbing materials like sandwiched foam composites and fabric can be used to dampen acoustical noise. Lining the inside wall of gradient tube and the magnet itself has been reported to absorb up to 23 dBA (28). The use of special fabric linings of magnet room walls can reduce sound levels by an additional 3 dBA (15, 28).
4. *Isolation by vacuum:* A vacuum around the gradient coil tube will reduce acoustic noise up to 23 dBA if the coil is independently supported (29).
5. *Passive damping by ear protection:* Earplugs attenuate 3–12 dBA, depending on the type used. Similar values can be obtained with earmuffs.
6. *Active noise cancellation:* Active noise cancellation can be performed using an acoustic environment antiphase signal (30). However, this method is of limited use in high field systems, because the generator for the antiphase noise is magnetic and it has to be in close proximity to the patient because of frequency dispersion of sound within the sound carrying tube. The use of a piezoelectric driver may be a solution; however, they have a limited bandwidth and the wires could interfere with the RF performance because of proximity. One vendor (Table 1, vendor 22) offers a system with 30-dB active noise cancellation in conjunction with an audio entertainment and communication

system with a high bandwidth. Other vendors (Table 1, vendors 13, 14, and 28) offer integrated noise reduction integrated into their RF coils.

Peripheral Nerve Stimulation. fMRI data are usually obtained with the use of ultrafast MRI sequences, such as echo-planar or spiral imaging. These sequences, to one degree or another, push the gradients to the limit of their performance, requiring rapid switching from positive to negative (and vice versa) peak amplitudes that translate in strong field variations (dB/dt). The rapidly switched gradient fields induce electric fields in the subject, which may cause an effect called peripheral nerve stimulation (PNS) (31). The level of stimulus depends on the peak amplitude and slew rate (dB/dt) of the gradients; the position of the subject in the magnet; and the weight, height, and conductivity of the subject (32, 33). Sensation varies from mild to painful or intolerable muscle contractions in different subjects (33–35). Because of the incommodious sensation and involuntary muscle twitching, PNS can severely affect and degrade the quality of fMRI data and therefore must be precluded from occurring. Several studies have been devoted to better characterizing PNS in the MRI environment (32–36). Such characterization is important not only to enable MRI operators to predict and avoid exposure of their subjects to any unwanted degree of PNS but also to allow regulatory agencies to express limits of safe operation of gradient systems (36). In addition, studies of gradient-induced PNS may enable gradient manufacturers to improve gradient coil design without inducing PNS (37, 38).

RF Coil Issues

There are a number of coil arrangements used in fMRI applications. For MRI systems with a single receiver, the major configurations are transmit and receive (transceive) volume coils (e.g., head coils), transceive linear or quadrature surface coils (partial volume coils), and transmit-only coils combined with receive-only coils (TORO). In TORO assemblies, volume transmit coils, such as whole-body resonators (39) or head coils (40), are used to produce a homogeneous B_1 field over the region of interest. Alternatively, partial-volume coils can also be used as transmit-only coils if they produce a fairly homogeneous field over the region of interest. The receive-only coil should be a single or quadrature surface coil.

Figure 4 shows examples of a variety of fMRI RF coils built for different purposes. Whole brain coils, such as the one shown in Figure 4(A), are small head

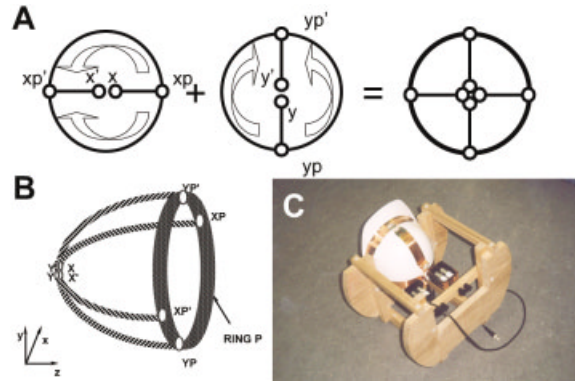


Figure 6 A helmet transceive quadrature coil for fMRI investigations of the motor cortex. The coil wires are attached to a safety helmet. This coil exhibits increased sensitivity at the top of the head where homogeneous head coils typically lack performance. (A) The principle of this helmet coil is based on split currents that are 90° out of phase, each from x and y at points x_p and y_p , respectively, with ring currents at x_p' and y_p' returning to x' and y' , respectively, as indicated by the arrows. (B) A 3-D schematic diagram of the current paths. (C) An experimental prototype coil built for 3 T. [Color figure can be viewed in the online issue, which is available at www.interscience.wiley.com.]

coils optimized for fMRI studies with a particular emphasis on correcting the sensitivity fall-off on the superior portion of the brain. The coil shown in Figure 4(A) consists of a whole-brain coil with a removable face coil, resulting in a high performance arrangement for the entire head that provides a high SNR and that is compatible with parallel imaging. The assembly reduces to a standard fMRI brain coil when the face coil is removed. Partial volume coils, such as the ones shown in Figure 4(B,C), have the advantage of providing good homogeneity and sensitivity over a smaller region of the brain. Local area brain coils are a good choice for fMRI experiments in single receiver MR systems. Local coils can be used either in transceive mode or as electronically decoupled receive coils in TORO arrangements. Utilizing brain array receive coils, such as the one shown in Figure 4(D), instead of whole-head coils leads to a further improvement of the SNR in the region of interest without compromising whole-brain coverage. It is advantageous to use dedicated local coils for increased sensitivity when doing fMRI paradigms targeted on known sites of functional activity (2, 41–43). Examples of such coils are shown in Figures 6 and 7. A quadrature helmet transceive coil (Fig. 6) was used to study function in the primary motor cortex (42, 43), because it has excellent sensitivity in the superior part of the human brain. An intrinsically decoupled quadrature coil assembly (Fig. 7) composed of a sin-

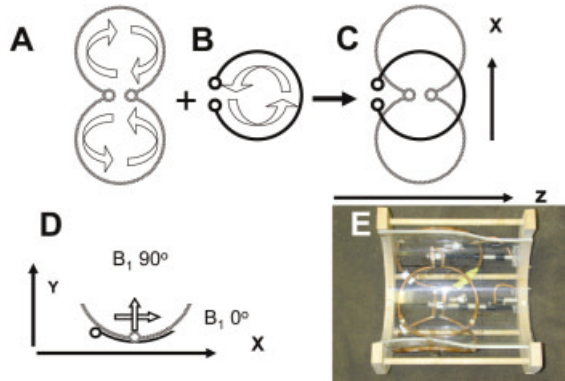


Figure 7 An experimental quadrature transceive coil assembly for fMRI experiments of the cerebellum. The assembly consists of (A) a coplanar dual loop coil and (B) a surface coil. (C) Both coils of the assembly are mounted on the surface of a cylindrical former and are combined with a 90° hybrid for quadrature mode. (D) An axial view with the indicated RF fields (arrows). (E) The verified experimental coil assembly built for 4 T. [Color figure can be viewed in the online issue, which is available at www.interscience.wiley.com.]

gle surface coil and a dual loop surface coil was used for a maximum sensitivity study of motor function in the cerebellum (44) and auditory function in Broca's area (45).

The development of multiple receiver MRI systems has dramatically extended the choices for TORO coil systems (46–49). Figure 8 shows examples of brain array coils for TORO imaging. Further sensitivity improvements are obtained with phased-array coils in combination with parallel imaging techniques, such as SMASH, SENSE, or similar approaches (50–53). In order to utilize the above techniques, good decoupling between the coil elements is a key requirement. Figure 9 shows an example of a four-element gapped receive array, which is improperly decoupled in Figure 9(A) and properly decoupled in Figure 9(B) using ultralow impedance preamplifiers. Decoupling principles for multiple-coil arrangements, including preamplifier decoupling, have allowed a more liberal coil arrangement and combination without the disadvantage of mutual coupling (54, 55, 64). This has allowed substantial improvements in the SNR when compared to using transceive schemes, as shown in Figure 10.

Peripheral Equipment Compatibility

The MRI scanner room is filled with a number of pieces of essential peripheral equipment to support the experiment or clinical exam being performed. In both the clinical and research environments, several de-

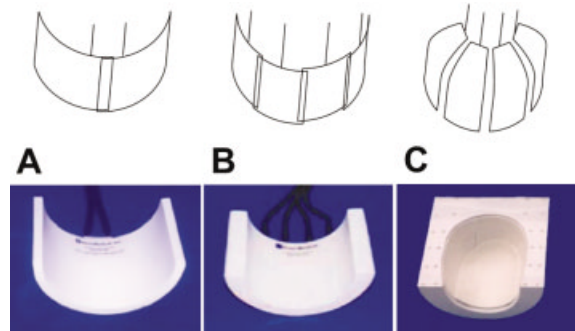


Figure 8 Commercially available receive arrays inserts for TORO (functional) imaging of the posterior brain. The RF is transmitted using a standard head coil (not shown). During transmission of the RF, the receive coils are electronically detuned. The shape, size, and number of elements in each coil are varied to optimize coverage over the area of interest or to utilize available system capabilities. For example, if there is only one receiver channel available then (A) a two-loop overlapped array for cerebellum studies can be combined using a quadrature hybrid and the resulting signal is fed to the receiver. (B) A four-channel receiver assembly for cerebellum or temporal lobe studies. Decoupling is partially achieved by overlap (nulling of the RF flux of adjacent loops). Additional decoupling is obtained using preamplifiers. (C) A gapped four-channel array for studies of the visual cortex. Decoupling is fully accomplished using preamplifiers. Pictures courtesy of NOVA Medical Inc. (Table 1, vendor 18). [Color figure can be viewed in the online issue, which is available at www.interscience.wiley.com.]

VICES are arranged near or around the MRI scanner. These include physiological monitoring devices, such as pulse oximeters, capnometers, electrocardiogram (ECG) monitors, temperature monitors, blood pres-

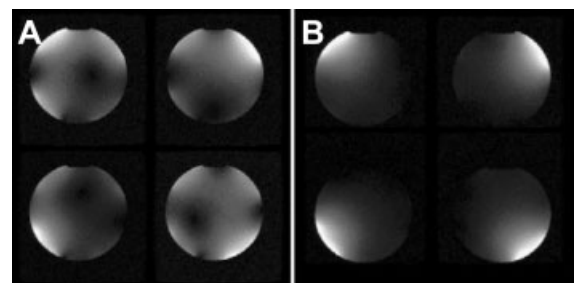


Figure 9 Axial images of a spherical phantom, showing the influence of preamplifier decoupling with a four-channel gapped receive array. (A) A low-impedance (5Ω) preamplifier was used. The intensity distribution shows significant interactions between the different channels. (B) The preamplifiers were replaced with ultralow impedance ($<1 \Omega$). No noticeable cross-talk can be observed between the receive arrays after this modification. Images courteously supplied by NOVA Medical Inc. (Table 1, vendor 18).

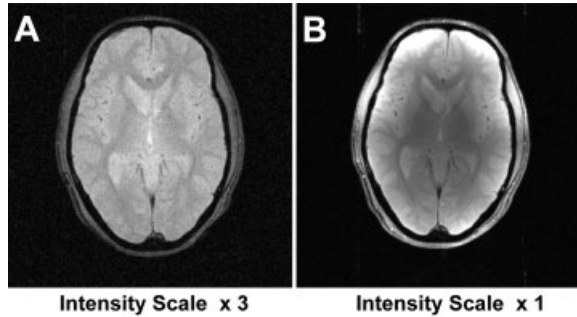


Figure 10 A SNR comparison at 1.5 T showing the advantages of multiple-receiver coils. (A) An optimized conventional image as obtained using a commercial standard head coil in quadrature mode. The image intensity is scaled by a factor 3 to show the fine details more clearly. (B) The same slice as obtained with the optimized parallel imaging technique using an eight-channel gapped receive array with preamplifier decoupling. The increases in the SNR are evident from the image. Images courtesy of Dr. Jacco de Zwart, National Institute of Neurological Disorders and Stroke, NIH (Bethesda, MD).

sure monitors, eye and respiratory motion detectors, and so forth; life support machines, such as artificial ventilators and anesthesia machines; functional stimulation equipment, such as video projectors, LED goggles, voltage and current stimulators, headphones, joysticks, and so forth; and entertainment and comforting equipment, such as video-cassette players and stereo sound systems. This equipment has to operate properly and safely in a high magnetic field environment. Therefore, significant constraints arise in their design and fabrication, as well as in their placement close to the magnet, to ensure MRI compatibility.

An example of peripheral equipment that is routinely used with fMRI experiments is the eye tracking system. Eye tracking is a method that monitors whether the subject has performed the task adequately during the entire experimental session. Information from the eye tracking system can be used to perform postprocessing correction, including discarding part or all of the data obtained. There are commercially available systems (Table 1, vendors 1 and 8). Additional examples of peripheral equipment include hardware approaches to observe head movement of the subject and to adjust image acquisition instantly using feedback circuitry for the gradient hardware (56).

Safety Issues. Perhaps the biggest concern when dealing with peripheral equipment in the MRI scanner room refers to their proximity to the magnet. At high magnetic fields of 1.5 T and above, equipment containing magnetic materials or parts can be pulled into

the magnet by unbearable forces, representing an enormous threat to the operator and especially to the patient or subject inside the magnet, should that equipment be allowed to come too close to the magnet. This is one of the greatest design constraints for MRI compatible equipment: they should contain as little as possible or no magnetic material. For example, equipment containing power transformers or magnetic cases should not be placed close to the magnet. Carts should be made of plastic, aluminum, or stainless steel. Nonmagnetic batteries should power portable and miniaturized equipment to prevent them from slipping out of the operator's hands and being pulled into the magnet bore.

The use of patient monitoring equipment with electrically conductive cables also creates a hazard for the patient. When a conductive cable is inserted into the bore of the magnet, a potential for patient burns exists. Hundreds of patient burns have occurred during MRI. Whenever conductive wires need to be brought into the magnet, it is essential that they are laid straight without loops and positioned as far from the RF coil and patient as possible to avoid acting as an RF antenna. The most frequently reported burn is at ECG electrode sites, which is caused by heat generated by electrical current flowing into the electrodes. The current is generated by the ECG patient cable, which acts as an antenna in the RF field of the MR scanner. New patient monitors, which incorporate fiber optics for monitoring ECG, eliminate the risk of patient burns. Fiber optic cables can also be used with thermometers and pulse oximeters and have the additional advantage of not bringing RF noise from outside into the magnet.

Reliability Issues. Many peripheral devices have small pumps and motors that are strongly affected by the high magnetic field environment. These types of equipment need to be positioned far from the magnet so that they can operate reliably. For equipment that does not require being immediately close to the patient or subject (such as the video projector, the video-cassette recorder, and the stereo system) this may not represent a drawback, because they can be located outside the RF room. However, for devices such as artificial ventilators and capnometers, the long distance between the device and the subject has disadvantages. These devices are usually designed to operate close to the patient or subject, and the large dead volume imposed by the long air tubes may prevent them from working properly. Volume-driven ventilators perform better than their pressure-driven counterparts when the air tube is more than 3 ft long. Alternatively, magnetic shielding can be used to protect the

equipment, which in turn makes this equipment magnetic and, as a result, turns it into a possible hazard. Consequently, it has to be mechanically fixed so can it can no longer cause danger to the subject or the operator.

Interference with MR Signals. Peripheral equipment should not interfere with the MR data acquisition. There are two major sources of interference. The first one is when a conductive wire placed inside the magnet bore brings RF noise from outside. The noise is picked up by the RF coil and digitized together with the MR signal, leading to a poor SNR and spikes in the MR images. Proper RF shielding and filtering of all conductive cables entering the magnet bore can prevent this source of interference. The second source of interference occurs when the conductive wire couples with the RF coil and “steals” the RF power transmitted to the coil. In this case, the area to be imaged does not see the intended excitation pulse and dark bands show up in the corresponding images. This problem can be avoided if the conductive wires are not close to the RF coil or if fiber optic cables replace them.

Dedicated fMRI Systems for Human Research

To date, the majority of fMRI experiments are conducted using clinical high field scanners (previously 1.5 T and now 3 T). These systems come configured for a broad range of applications and fMRI capability is an optional feature, not the main purpose of the instrument. Nevertheless, with the explosion of fMRI as a major brain research tool, more and more dedicated fMRI systems for human research are becoming available with field strengths varying from 3 to 9.4 T. Dedicated brain scanners can be acquired (Table 1, vendor 25), as can fMRI research systems (Table 1, vendor 30). Comprehensive clinical fMRI packages include an RF coil with a headset and mirror, as well as software and hardware for paradigm presentation, physiological monitoring, motion correction and data analysis (Table 1, vendor 14).

Dedicated Nonhuman Primate fMRI Systems

Animal-based fMRI research has been able to take advantage of higher field strengths up to 11.7 T for improved spatial specificity and sensitivity. Dedicated nonhuman primate fMRI systems ranging from 4.7 to 9.4 T in horizontal and vertical configurations have

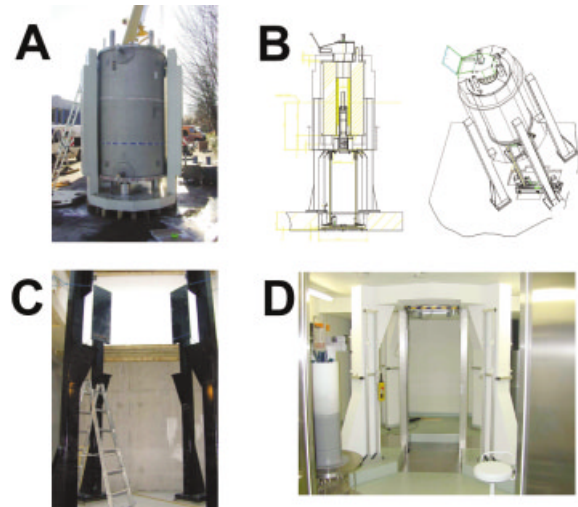


Figure 11 The 7-T 600-mm vertical bore dedicated fMRI magnet for nonhuman primate studies. (A) The magnet during installation (iron shield under construction). (B) A schematic drawing of the setup. (C) The support legs during construction. (D) The installed magnet with details of the monkey chair shown on the left side. [Color figure can be viewed in the online issue, which is available at www.interscience.wiley.com.]

become available in several neuroscience laboratories throughout the world. These systems can be purchased as a closed, complete package (Table 1, vendor 2) or assembled in the laboratory from specific components acquired for the specific purpose of performing fMRI. The first dedicated nonhuman primate fMRI system was installed in 1997 at the Max-Planck Institute for Biological Cybernetics in Tübingen, Germany (Fig. 11). Since then, outstanding fMRI results using a vertical magnet system have been published (57–60). This dedicated vertical system, which is designed for macaque monkeys, is equipped with a chair for the animal like the one used for electrophysiological studies, including the head fixture. The chair is mounted on a hydraulic lift for transporting the animal and the electronic setup to the magnet center. Functional experimental protocols have been worked out for awake or anesthetized monkeys (57). A series of customized RF coils were developed for the purpose of global brain studies in macaques and for dedicated fMRI studies of the monkey visual system (60). The homogeneous RF coils are being used for high-resolution anatomical imaging experiments for localizing and differentiating tissue, measuring brain volume, and rendering of the skull. Skull rendering gives 3-D information that can be used for custom manufacturing of implants for individual animals.

FUTURE DIRECTIONS FOR fMRI HARDWARE DEVELOPMENT

The past decade has been called the *decade of the brain* but might as well have been called the *era of fMRI*. The most important brain research tool today is fMRI, and it has served as strong motivation for continued technological improvements in MRI hardware. Both BOLD-based and CBF-based fMRI techniques greatly benefit from higher magnetic fields, which provide a higher SNR, a higher CNR, and better spatial localization.

The use of high magnetic fields brings many problems that call for interesting hardware solutions. There is an increased demand on gradient performance, thus escalating the problems associated with acoustical noise and PNS. New gradient designs must incorporate acoustics as a parameter (20). Making gradient coils that are targeted to act only over the region of interest may be a possible solution for avoiding PNS (35, 61–63). The increased bandwidth associated with higher gradient performance, as well as the increased physiological noise, reduce the net gain in the SNR, calling for creative RF coil designs that limit the tissue contribution to thermal noise. With the sharp technological developments in electronics, modern MRI spectrometers now come equipped with multiple receiver units, thereby allowing parallel acquisition of data. The combination of small, multielement receive-only RF coils with parallel imaging techniques is changing the way MRI data are acquired. By reducing the coil size, data from a small local region can be acquired with much higher sensitivity because of the close proximity of the coil to the region of interest and the limited noise contribution from tissue. Tissue coverage is achieved with the use of multiple elements, which are decoupled from each other by a modern combination of electronic detuning with high-impedance preamplifiers. At the time of writing this article new MRI consoles can be equipped with as much as 8 receivers and the expansion to 16 or even 32 is already in the plans. One problem associated with parallel imaging refers to the storage and processing of a much larger amount of data. Therefore, considerable effort must be put into increasing the processing capabilities of array processors, as well as boosting the data transfer rate so that images can be continuously updated on the display and stored to media without imposing significant limitations to fMRI paradigms. Finally, pulse sequence design at high magnetic fields must account for the decreased contrast in relaxation times, in-

creased chemical shift, susceptibility artifacts, and the limitations in RF power deposition.

REFERENCES

1. Bandettini PA, Wong EC, Hinks RS, Tikofsky RS, Hyde JS. Time course EPI of human brain function during task activation. *Magn Reson Med* 1992; 25: 390–397.
2. Ogawa S, Tank DW, Menon RS, Ellermann JM, Kim S-G, Merkle H, Ugurbil K. Intrinsic signal changes accompanying sensory stimulation: Functional brain mapping with magnetic resonance imaging. *Proc Natl Acad Sci USA* 1992; 89:5951–5955.
3. Kim SG. Quantification of relative cerebral blood flow change by flow-sensitive alternating inversion recovery (FAIR) technique: Application to functional mapping. *Magn Reson Med* 1995; 34:293–301.
4. Kwong KK, Chesler DA, Weisskoff RM, Donahue KM, Davis TL, Ostergaard L, Campbell TA, Rosen BR. MR perfusion studies with T1-weighted echo planar imaging. *Magn Reson Med* 1995; 34:878–887.
5. Belliveau JW, Rosen BR, Kantor HL, Rzedzian RR, Kennedy DN Jr, McKinstry RC, Vevea JM, Cohen MS, Pykett IL, Brady TJ. Functional cerebral imaging by susceptibility-contrast NMR. *Magn Reson Med* 1990; 14:538–546.
6. Glover GH. Hardware for functional MRI. In: Jezzard P, Matthews PM, Smith SM, editors. *Functional MRI: An introduction to methods*, 1st ed. Oxford: Oxford University Press; 2001. p 109–122.
7. Gruetter R. Automatic, localized in vivo adjustment of all first- and second-order shim coils. *Magn Reson Med* 1993; 29:804–811.
8. Turner R. Gradient coil design: A review of methods. *Magn Reson Imaging* 1993; 11:903–920.
9. Redpath TW. Signal-to-noise ratio in MRI. *Br J Radiol* 1998; 71(847):704–707.
10. Gati JS, Menon RS, Ugurbil K, Rutt BK. Experimental determination of the BOLD field strength dependence in vessels and tissue. *Magn Reson Med* 1997; 38:296–302.
11. Collins CM, Li S, Smith MB. SAR and B1 field distributions in a heterogeneous human head model within a birdcage coil. Specific energy absorption rate. *Magn Reson Med* 1998; 40:847–856.
12. Collins CM, Smith MB. Signal-to-noise ratio and absorbed power as functions of main magnetic field strength, and definition of “90 degrees” RF pulse for the head in the birdcage coil. *Magn Reson Med* 2001; 45:684–691.
13. Vaughan JT, Garwood M, Collins CM, Liu W, Delabarre L, Adriany G, Anderson P, Merkle H, Goebel R, Smith MB, Ugurbil K. 7T vs. 4T: RF power, homogeneity, and signal-to-noise comparison in head images. *Magn Reson Med* 2001; 46:24–30.
14. Hedeem RA, Edelstein WA. Characterization and pre-

- diction of gradient acoustic noise in MR imagers. *Magn Reson Med* 1997; 37:7–10.
15. Mechefske CK, Geris R, Gati JS, Rutt BK. Acoustic noise reduction in a 4 T MRI scanner. *MAGMA* 2002; 13:172–176.
 16. Bandettini PA, Jesmanowicz A, Van Kylen J, Birn RM, Hyde JS. Functional MRI of brain activation induced by scanner acoustic noise. *Magn Reson Med* 1998; 39:410–416.
 17. Talavage TM, Edmister WB, Ledden PJ, Weisskoff RM. Quantitative assessment of auditory cortex responses induced by imager acoustic noise. *Hum Brain Mapp* 1999; 7:79–88.
 18. Shah NJ, Jancke L, Grosse-Ruyken ML, Muller-Gartner HW. Influence of acoustic masking noise in fMRI of the auditory cortex during phonetic discrimination. *J Magn Reson Imaging* 1999; 9:19–25.
 19. Hall DA, Summerfield AQ, Goncalves MS, Foster JR, Palmer AR, Bowtell RW. Time-course of the auditory BOLD response to scanner noise. *Magn Reson Med* 2000; 43:601–606.
 20. Edelstein WA, Hedeem RA, Mallozzi RP, El Hamamsy SA, Ackermann RA, Havens TJ. Making MRI quieter. *Magn Reson Imaging* 2002; 20:155–163.
 21. Loenneker T, Hennel F, Ludwig U, Hennig J. Silent BOLD imaging. *MAGMA* 2001; 13:76–81.
 22. Oesterle C, Hennel F, Hennig J. Quiet imaging with interleaved spiral read-out. *Magn Reson Imaging* 2001; 19:1333–1337.
 23. Bowtell RW, Mansfield P. Quiet transverse gradient coils: Lorentz force balanced designs using geometrical similitude. *Magn Reson Med* 1995; 34:494–497.
 24. Mansfield P, Chapman BL, Bowtell R, Glover P, Coxon R, Harvey PR. Active acoustic screening: Reduction of noise in gradient coils by Lorentz force balancing. *Magn Reson Med* 1995; 33:276–281.
 25. Mansfield P, Glover PM, Beaumont J. Sound generation in gradient coil structures for MRI. *Magn Reson Med* 1998; 39:539–550.
 26. Mansfield P, Haywood B. Principles of active acoustic control in gradient coil design. *MAGMA* 2000; 10:147–151.
 27. Mansfield P, Haywood B, Coxon R. Active acoustic control in gradient coils for MRI. *Magn Reson Med* 2001; 46:807–818.
 28. Moelker A, Maas RA, Lethimonnier F, Pattynama PM. Interventional MR Imaging at 1.5 T: Quantification of sound exposure. *Radiology* 2002; 224:889–895.
 29. Katsunuma A, Takamori H, Sakakura Y, Hamamura Y, Ogo Y, Katayama R. Quiet MRI with novel acoustic noise reduction. *MAGMA* 2002; 13:139–144.
 30. McJury M, Stewart RW, Crawford D, Toma E. The use of active noise control (ANC) to reduce acoustic noise generated during MRI scanning: Some initial results. *Magn Reson Imaging* 1997; 15:319–322.
 31. Cohen MS, Weisskoff RM, Rzedzian RR, Kantor HL. Sensory stimulation by time-varying magnetic fields. *Magn Reson Med* 1990; 14:409–414.
 32. Ham CL, Engels JM, van de Wiel GT, Machielsen A. Peripheral nerve stimulation during MRI: Effects of high gradient amplitudes and switching rates. *J Magn Reson Imaging* 1997; 7:933–937.
 33. Bourland JD, Nyenhuis JA, Schaefer DJ. Physiologic effects of intense MR imaging gradient fields. *Neuroimaging Clin N Am* 1999; 9:363–377.
 34. Budinger TF, Fischer H, Hentschel D, Reinfelder HE, Schmitt F. Physiological effects of fast oscillating magnetic field gradients. *J Comput Assisted Tomogr* 1991; 15:909–914.
 35. Chronik BA, Rutt BK. A comparison between human magnetostimulation thresholds in whole-body and head/neck gradient coils. *Magn Reson Med* 2001; 46:386–394.
 36. Den Boer JA, Bourland JD, Nyenhuis JA, Ham CL, Engels JM, Hebrank FX, Frese G, Schaefer DJ. Comparison of the threshold for peripheral nerve stimulation during gradient switching in whole body MR systems. *J Magn Reson Imaging* 2002; 15:520–525.
 37. Harvey PR, Mansfield P. Avoiding peripheral nerve stimulation: Gradient waveform criteria for optimum resolution in echo-planar imaging. *Magn Reson Med* 1994; 32:236–241.
 38. Harvey PR, Katznelson E. The modular gradient coil: A holistic approach to power efficient and high performance whole-body MRI without peripheral nerve stimulation. *MAGMA* 1999; 9:152–155.
 39. Hayes CE, Axel L. Noise performance of surface coils for magnetic resonance imaging at 1.5 T. *Med Phys* 1985; 12:604–607.
 40. Barfuss H, Fischer H, Hentschel D, Ladebeck R, Oppelt A, Wittig R, Duerr W, Oppelt R. In vivo magnetic resonance imaging and spectroscopy of humans with a 4 T whole-body magnet. *NMR Biomed* 1990; 3:31–45.
 41. Ogawa S, Menon RS, Tank DW, Kim SG, Merkle H, Ellermann JM, Ugurbil K. Functional brain mapping by blood oxygenation level-dependent contrast magnetic resonance imaging. A comparison of signal characteristics with a biophysical model. *Biophys J* 1993; 64:803–812.
 42. Kim SG, Ashe J, Hendrich K, Ellermann JM, Merkle H, Ugurbil K. Functional magnetic resonance imaging of motor cortex: Hemispheric asymmetry and handedness. *Science* 1993; 261(5121):615–617.
 43. Merkle H, Garwood M, Ugurbil K. Dedicated circularly polarized surface coil assemblies for brain studies at 4T. In: *Proceedings of the Society of Magnetic Resonance in Medicine Twelfth Annual Scientific Meeting*, New York, August 14, 1993. Vol. 3, p 1358.
 44. Ellerman JM, Flament D, Kim SG, Fu QG, Merkle H, Ebner TJ, Ugurbil K. Spatial patterns of functional activation of the cerebellum investigated using high field (4 T) MRI. *NMR Biomed* 1994; 7:63–68.
 45. Hinke RM, Hu X, Stillman AE, Kim SG, Merkle H, Salmi R, Ugurbil K. Functional magnetic resonance imaging of Broca's area during internal speech. *Neuroreport* 1993; 4:675–678.

46. Wald LL, Moyher SE, Day MR, Nelson SJ, Vigneron DB. Proton spectroscopic imaging of the human brain using phased array detectors. *Magn Reson Med* 1995; 34:440–445.
47. Wald LL, Carvajal L, Moyher SE, Nelson SJ, Grant PE, Barkovich AJ, Vigneron DB. Phased array detectors and an automated intensity-correction algorithm for high-resolution MR imaging of the human brain. *Magn Reson Med* 1995; 34:433–439.
48. Wright SM, Wald LL. Theory and application of array coils in MR spectroscopy. *NMR Biomed* 1997; 10: 394–410.
49. Wald LL, Frederick B, Renshaw PF. NAA-weighted imaging of the human brain using a conventional read-out gradient. *Magn Reson Med* 1999; 41:187–192.
50. Pruessmann KP, Weiger M, Scheidegger MB, Boesiger P. SENSE: Sensitivity encoding for fast MRI. *Magn Reson Med* 1999; 42:952–962.
51. Sodickson DK, Griswold MA, Jakob PM. SMASH imaging. *Magn Reson Imaging Clin N Am* 1999; 7:237.
52. Madore B, Glover GH, Pelc NJ. Unaliasing by Fourier-encoding the overlaps using the temporal dimension (UNFOLD), applied to cardiac imaging and fMRI. *Magn Reson Med* 1999; 42:813–828.
53. Kellman P, Epstein FH, McVeigh ER. Adaptive sensitivity encoding incorporating temporal filtering (TSENSE). *Magn Reson Med* 2001; 45:846–852.
54. Roemer PB, Edelstein WA, Hayes CE, Souza SP, Mueller OM. The NMR phased array. *Magn Reson Med* 1990; 16:192–225.
55. Sodickson DK, McKenzie CA, Ohliger MA, Yeh EN, Price MD. Recent advances in image reconstruction, coil sensitivity calibration, and coil array design for SMASH and generalized parallel MRI. *MAGMA* 2002; 13:158–163.
56. Norris DG, Driesel W. Online motion correction for diffusion-weighted imaging using navigator echoes: Application to RARE imaging without sensitivity loss. *Magn Reson Med* 2001; 45:729–733.
57. Logothetis NK, Guggenberger H, Peled S, Pauls J. Functional imaging of the monkey brain. *Nature Neurosci* 1999; 2:555–562.
58. Logothetis N. Can current fMRI techniques reveal the micro-architecture of cortex? *Nature Neurosci* 2000; 3:413–414.
59. Logothetis NK, Pauls J, Augath M, Trinath T, Oeltermann A. Neurophysiological investigation of the basis of the fMRI signal. *Nature* 2001; 412(6843): 150–157.
60. Logothetis N, Merkle H, Augath M, Trinath T, Ugurbil K. Ultra high-resolution fMRI in monkeys with implanted RF coils. *Neuron* 2002; 35:227–242.
61. Abduljalil AM, Aletras AH, Robitaille PM. Torque free asymmetric gradient coils for echo planar imaging. *Magn Reson Med* 1994; 31:450–453.
62. Alsop DC, Connick TJ. Optimization of torque-balanced asymmetric head gradient coils. *Magn Reson Med* 1996; 35:875–886.
63. Crozier S, Doddrell DM. A simple design methodology for elliptical cross-section, transverse, asymmetric, head gradient coils for MRI. *IEEE Trans Biomed Eng* 1998; 45:945–948.
64. de Zwart JA, Ledden PJ, Kellman P, van Gelderen P, Duyn JH. Design of a SENSE-optimized high-sensitivity MRI receive coil for brain imaging. *Magn Reson Med* 2002; 47:1218–1227.
65. de Zwart J, van Gelderen P, Kellman P, Duyn J. Reduction of gradient acoustic noise in MRI using SENSE-EPI. *Neuroimage* 2002; 16:1151–1155.